Super-smooth surface fabrication technique and experimental research

Linghua Zhang,[1,*] Junlin Wang,[1] and Jian Zhang[2]

[1]The State Key Laboratory of Applied Optics, Changchun Institute of Optics, Fine Mechanics and Physics, Chinese Academy of Science, Changchun 130033, China

[2]Key Laboratory of Airborne Optical Imaging and Measurement, Changchun Institute of Optics, Fine Mechanics and Physics, Chinese Academy of Science, Changchun 130033, China

*Corresponding author: zhanglinghuahit@163.com

Received 12 June 2012; revised 21 August 2012; accepted 22 August 2012; posted 23 August 2012 (Doc. ID 170269); published 18 September 2012

Wheel polishing, a new optical fabrication technique, is proposed for super-smooth surface fabrication of optical components in high-precision optical instruments. The machining mechanism and the removal function contours are investigated in detail. The elastohydrodynamic lubrication theory is adopted to analyze the deformation of the wheel head, the pressure distribution, and the fluid film thickness distribution in the narrow machining zone. The pressure and the shear stress distributions at the interface between the slurry and the sample are numerically simulated. Practical polishing experiments are arranged to analyze the relationship between the wheel–sample distance and the machining rate. It is demonstrated in this paper that the wheel–sample distance will directly influence the removal function contours. Moreover, ripples on the wheel surface will eventually induce the transverse prints on the removal function contours. The surface roughness of fused silicon is reduced to less than 0.5 nm (rms) from initial 1.267 nm (rms). The wheel polishing technique is feasible for super-smooth surface fabrication.

OCIS codes: 220.0220, 220.4610.

1. Introduction

In high precision optical instruments, an extremely smooth surface is demanding, especially for the projection lens of optical lithography [1–3]. Optical elements in these instruments mostly require subnanometer surface roughness without introducing subsurface damage. They are called super-smooth surfaces [4,5]. Three contributive techniques reported to apply for the super-smooth surface fabrication are float polishing, bowl polishing, and elastic emission machining. They are all noncontact polishing processes. The samples and the polishing tools are separated by the lubrication fluid film. Surface material is removed by the abrasives suspending in the slurry. Flat Zerodur surface with atomic size roughness (0.085 nm rms) is realized using the elastic emission machining by Kanaoka *et al.*[6] and Mori *et al.* [7].

Our research group presents wheel polishing based on the hydrodynamic lubrication theory. The machining mechanism is investigated and then the fluid film thickness and the pressure distributions in the machining zone are studied according to the elastohydrodynamic lubrication theory. The pressure and the shear stress distributions are obtained in numerical simulation and the results are compared with those that are theoretical. Experiments are arranged in order to get the removal function contours and verify the practical value of the wheel polishing. Effects of different factors are discussed and the wheel–sample distance is experimentally studied.

2. Wheel Polishing

The schematic diagram of wheel polishing is shown in Fig. 1. The rubber polishing wheel is immersed in

1559-128X/12/276612-06$15.00/0

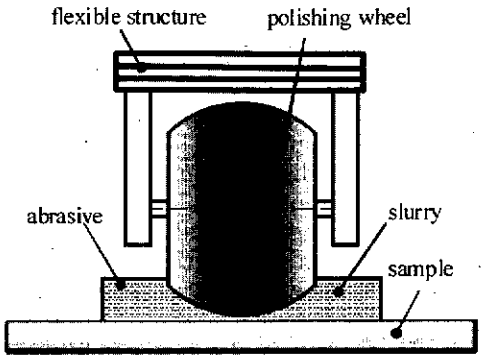

Fig. 1. (Color online) Machining mechanism schematic diagram of the wheel polishing.

the slurry and rotates around the horizontal axis. During the polishing process, abrasives suspended in the slurry are continuously dragged into the narrow converged polishing zone and the pressure rises sharply. Positive pressure is generated when the film thickness is diminishing. The polishing wheel floats above the sample surface when sufficient pressure is produced. The wheel reaches a balance position and a thin fluid film about several μm in thickness forms. This phenomenon is the hydrodynamic lubrication. Since the viscosity of the slurry is low, elastohydrodynamic lubrication appears only under the condition of high speed and light load. Outer surface atoms of the abrasives and the sample will react with each other, bond together, and finally leave the sample surface under the viscous drag effect of the fast flowing slurry.

The polishing wheel transmits energy to the slurry by high-speed rotation. The slurry is considered a uniform and stable liquid. It is believed that the abrasives and the slurry move together and have the same velocity. The sample is static. The velocity gradient forms at the interface between the abrasives and the sample and leads to the shear stress distribution at the interface. The shear stress may be large enough to break the bonding force between the surface atoms and the sublayer surface atoms of the sample. Eventually, the surface atoms are dragged away and leave the sample surface.

Generally, the shear stress distribution is a critical factor of the removal process. We can analyze the removal opportunity and the machining rate distribution by analyzing the shear stress distribution at the interface between the abrasives and the sample.

3. Elastohydrodynamic Lubrication

The slurry is compressed in the converged machining zone. The viscosity of the slurry will increase sharply to resist the compression. Meanwhile, the pressure will simultaneously increase due to the viscosity-pressure effect [8]. The wheel is made of soft rubber. It will distort itself and float above the sample.

The elastohydrodynamic lubrication is applied here in the point contact lubrication state of the polishing wheel and the flat sample surface.

The fluid film thickness can be expressed by the deformation of the wheel head (d), the initial fluid film thickness (h_0) and the sample-wheel distance (s) as

$$h(x,y) = h_0 + s(x,y) + d(x,y)$$
$$s(x,y) = \frac{x^2}{2R} + \frac{y^2}{2R}, \quad (1)$$

where h is the fluid film thickness. R is the radius of curvature.

The isograms of the wheel–sample distance are a series of circles. Therefore the profile of the fluid film thickness will be a round shape after the deformation.

The Reynolds equation is adopted here to show the relationship between the film thickness and pressure, the following equation is obtained

$$3h^2\frac{\partial h}{\partial x}\frac{\partial p}{\partial x} + h^3\frac{\partial^2 p}{\partial x^2} + 3h^2\frac{\partial h}{\partial y}\frac{\partial p}{\partial y} + h^3\frac{\partial^2 p}{\partial y^2} = 6\mu U\frac{\partial h}{\partial x}, \quad (2)$$

where U is the peripheral velocity of the polishing wheel surface.

Otherwise, the stress-strain equation in Eq. (3) shows the relationship between the deformation of the wheel head and the pressure. It can be described as

$$d(x,y) = \frac{2}{\pi E}\iint_A \frac{p(x',y')dx'dy'}{\sqrt{(x'-x)^2 + (y'-y)^2}}, \quad (3)$$

where E is the elastic modulus of the rubber rotating wheel head.

Generally, the fluid film thickness (h), the pressure (p) and the deformation of the wheel head (d) can all be calculated according to Eqs. (1)–(3). Direct solution of the elastohydrodynamic lubrication is difficult. Experimental and numerical solutions for the elastohydrodynamic lubrication have been researched by many scientists.

The deformation of the wheel head is shown in Fig. 2. The horizontal axis presents the slurry motion direction. The inlet area is on the left. The deformation of the inlet area is larger than the back outlet.

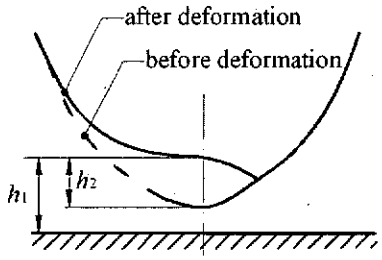

Fig. 2. Deformation of the wheel: h_1 is the total deformation amount and h_2 is the wheel deformation amount. The fluid film thickness is $h_1 - h_2$.

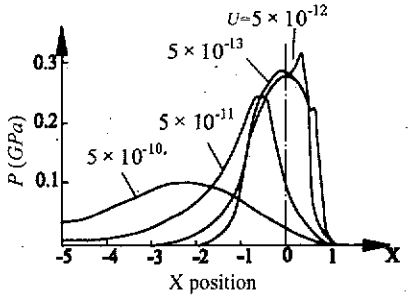

Fig. 3. Pressure distribution for different rotating parameters. (The x axis represents the normalized position in the direction of slurry motion.)

The pressure distribution in the direction of the slurry motion has been researched by Peiran *et al.* [9] as shown in Fig. 3. In contrast to the deformation profile in Fig. 2, it can be concluded that the pressure rises with the shrinking of the polishing zone. The pressure increases to its maximum value then falls with the enlarging of the polishing zone.

The pressure distribution has two kinds of profiles. It has one smooth peak under the condition of high speed or low load and another sharp, lower peak near the outlet area under the condition of low speed or high load.

The fluid film thickness distribution is shown in Fig. 4. It is experimentally researched by Zhu *et al.* [10]. The fluid film-thickness distribution is similar a horse shoe. The thinnest area of the fluid film thickness appears on two sides of the wheel head. The profile of the fluid film thickness is round.

4. Numerical Simulation

The removal of material is attributed to the shear stress at the interface between the abrasives and the sample. Abrasives are suspended in the slurry. It is difficult to analyze the distribution of the abrasives or drive their injection direction directly. The slurry is considered a uniform and stable liquid. The abrasives move together with the slurry so the kinematic parameters of the slurry are analyzed instead of that of the abrasives. The flow within the lubrication fluid film layer is laminar. It is believed that the pressure doesn't change in the thickness direction [11]. The physical model is established. A wheel rotates at 300 rpm against a flat plate immersed in fluid. The distance between the wheel and the plate is 5 μm. The deformation of the wheel is not considered here.

The simulation solutions of the dynamic pressure and the shear stress distributions are shown in Fig. 5. The pressure distribution has one global peak and rises up until it reaches the peak and then falls down sharply. The shape is similar to the theoretical profile under high speed or light load analyzed before. The shear stress in the polishing direction has a smooth profile that is similar to that of the pressure distribution.

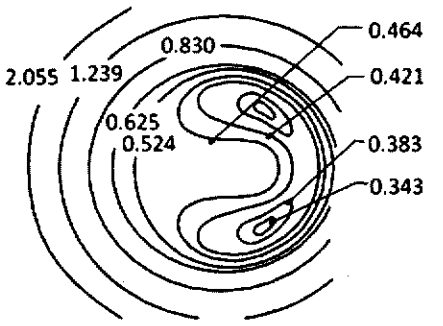

Fig. 4. Fluid film thickness (unit: micrometers) distribution in the parallel surface of the sample surface [10].

5. Experiments and Discussion

Practical polishing experiments are arranged. It is proposed that the machining rate is proportional to the shear stress at the interface between the abrasives and the sample. The shear stress is induced by the velocity gradient at the interface [12]. We have to figure out and properly control all the factors that influence the shear stress distribution at the interface during the whole super-smooth surface polishing process.

The influencing factors for the shear stress distribution generally include four groups. The first group includes the fluid film thickness and the rotating speed of the wheel. The second group consists of the slurry parameters such as viscosity, average

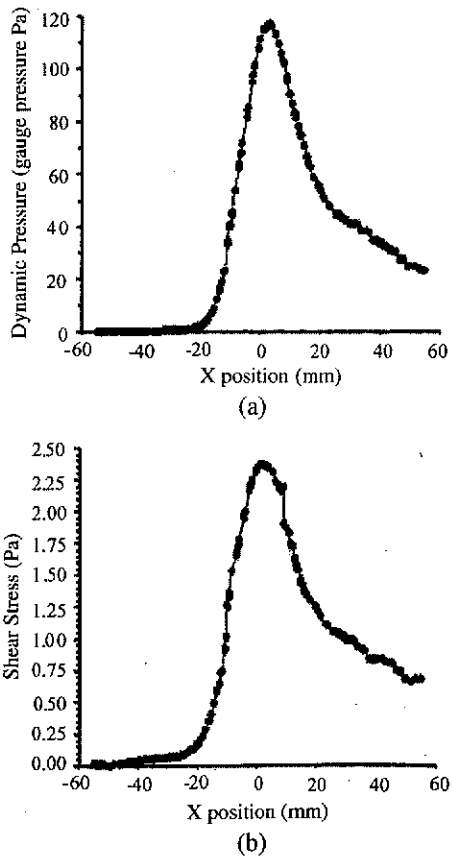

Fig. 5. (a) Dynamic pressure and (b) the shear stress distributions in the direction of slurry motion.

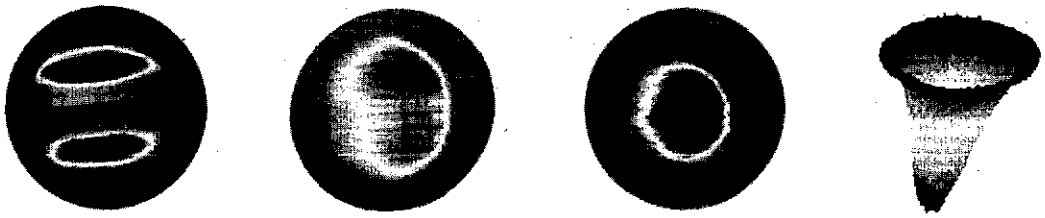

(a) (b) (c) (d)

Fig. 6. (Color online) Removal function contours of different wheel–sample distances (a) 0 μm, (b) 5 μm, and (c) 10 μm. (d) Vertical profile of the removal function contours of the 10 μm mode.

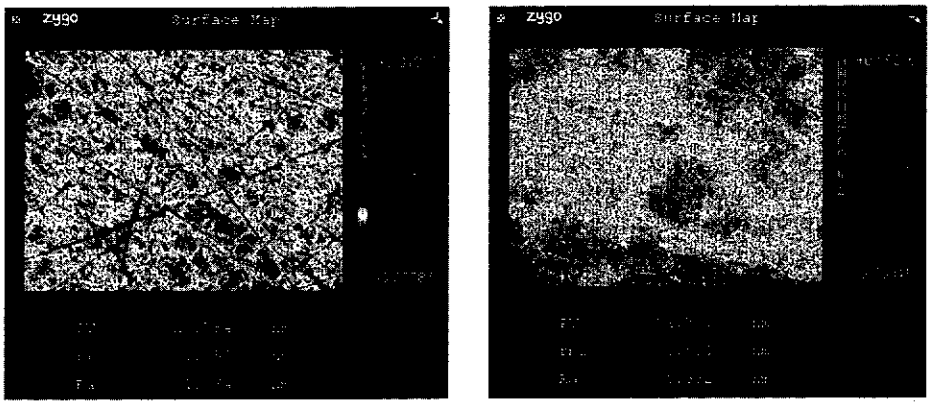

(a)

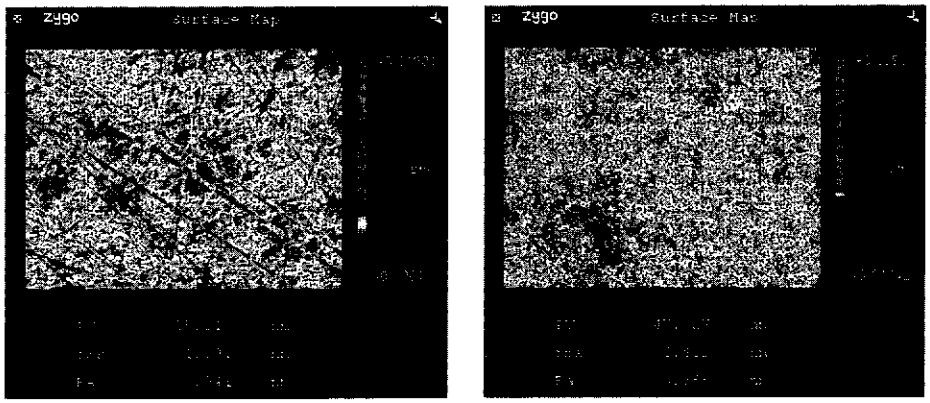

(b)

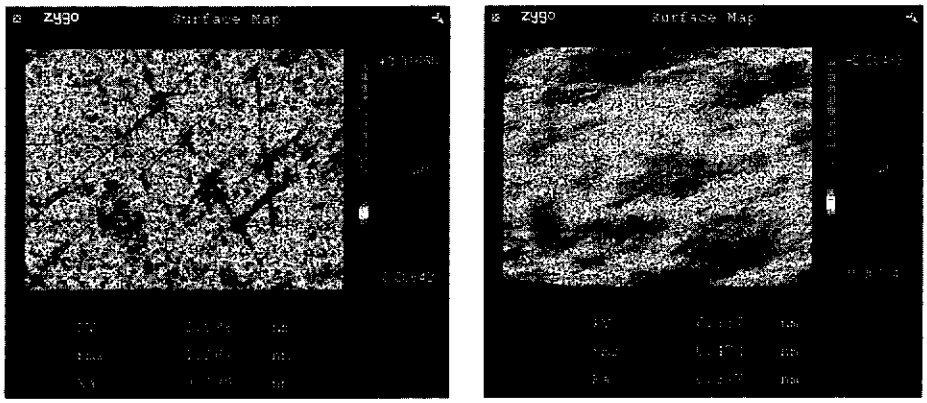

(c)

Fig. 7. (Color online) Surface roughness before and after being processed for different wheel–sample distances: (a) 0 μm, (b) 5 μm, and (c) 10 μm.

particles size, the mechanical and the chemical properties, and the volume fraction of abrasives. The third group is the parameters the polishing wheel, including the curvature, the surface roughness, the shape, and the elastic modular. The last group is the parameters of sample, including the chemical and the mechanical properties, the surface roughness, the ripple, and the geometry parameters.

The colloidal dioxide silicon is utilized as an abrasive in the slurry. The sample material is fused silica. The influence of the wheel–sample distance on the removal function contours is researched in detail. Three kinds of distance modes are studied: the contact mode 0, 5, and 10 μm. The same polishing wheel polishes the same material in the same speed (300 rpm) for 30 min. The surfaces processed are measured by the ZYGO interferometer. The removal function contours are shown in Fig. 6. The surface roughness before and after being processed is measured by the white light interferometer. The initial surface roughness is all larger than 1.0 nm (rms).

The removal function contours in Figs. 6(a) and 6(b) have a similar pattern with that of the fluid film thickness distribution in Fig. 4. They are both horse shoe shape and have two peaks. The two peaks join at the backward area. The removal function contour of the 10 μm mode tends to have a comparative convex shape and get the maximum value at the center of the machining zone.

It has been concluded that the material is all removed inside a circle. The surface roughness after being processed is measured for different zones. The average surface roughness is about 0.5 nm (rms) (shown in Fig. 7). The surface roughness is reduced to 0.472 nm (rms) while the wheel–sample distance is 10 μm.

All removal function contours have an inverse pattern as that of the fluid film thickness distribution that is also experimentally investigated by Su *et al.* [13] and Kaneta *et al.* [14]. The machining rate can be calculated through the removal amount divided by the processing time. The machining rate should have the same contours as the removal function contours. So, the machining rate also has an inverse pattern with that of the fluid film thickness distribution. The machining rate will get the maximum value in the thinnest fluid film zone. Above all, the wheel–sample distance is a critical factor influencing the lubrication state and the machining rate.

Otherwise, the transverse prints are found on the removal function contours. These prints are probably due to the surface ripples on the surface of the polishing-wheel head. The polishing head is made of the semispherical shape steel core and an outer elastic rubber layer that lies on surface of the wheel. The mold of the elastic rubber layer is manufactured in a lathe. The tool path brings longitude ripples on the mold. The ripples are then transmitted from the mold to the elastic rubber layer on the wheel. Finally the prints are observed on the surface of the removal function contours. The ripples directly change the wheel–sample distance. This change of the distance results in varying of the lubrication state and eventually the machining rate is influenced. On the other hand, the tiny difference in the machining rate accumulates with time.

6. Conclusion

In this study a new super-smooth polishing technique is introduced. It aims to analyze the machining mechanism based on the elastohydrodynamic lubrication theory, which is known as the common machining mechanism of elastic emission machining and float polishing. The relationship among the film thickness distribution, the wheel head deformation, and the pressure distribution are presented. The solution for the Reynolds equation, the stress-strain equation, and the deformation equation is experimentally researched in other fields. The pressure distribution in the polishing direction is numerical simulated and has a shape that is similar to the theoretical one under high speed or low load.

The profiles of the removal areas are all round in shape. The convex removal function contour is obtained when the wheel–sample distance is 10 μm. The horseshoe shape contours are obtained for 5 μm and the contact modes. The removal function contours all have an inverse pattern of the fluid film thickness distribution. The surface roughness is reduced to less than 0.5 nm (rms) from more than 1.0 nm (rms). The transverse prints that appear on the removal function contours are due to ripples of the polishing wheel surface.

I am deeply grateful to my colleagues, who cooperated with me to carry out the experiments, and also the State Key Laboratory of Applied Optics. All research was assisted through funds from the Key Program of the Major Subject of National Science and Technology.

References

1. T. Miura, K. Murakami, K. Suzuki, Y. Kohama, K. Morita, K. Hada, and Y. Ohkubo, "Nikon EUVL development progress update," Proc. SPIE **6517**, 651707 (2007).
2. M. Ando, M. Negishi, M. Takimoto, A. Deguchi, and N. Nakamura, "Super-smooth polishing on aspherical surfaces," Nanotechnology. **6**, 111–120 (1995).
3. M. Ando, M. Negishi, M. Takimoto, A. Deguchi, N. Nakamura, M. Higomura, and H. Yamamoto, "Super-smooth surface polishing on aspherical optics," Proc. SPIE **1720**, 22–23 (1992).
4. H. Gao, J. Cao, M. Wu, Y. Zhu, and C. Chen, "Process technology for supersmooth surface machining," Proc. SPIE **4231**, 208–213 (2000).
5. J. R. Arthur and R. O. Tatchyn, "Radiation properties of the Linac coherent light source: Challenges for x-ray optics," Proc. SPIE **4143**, 1–8 (2001).
6. M. Kanaoka, H. Takino, K. Nomura, Y. Mori, H. Mimura, and K. Yamauchi, "Removal properties of low-thermal-expansion materials with rotating-sphere elastic emission machining," Sci. Technol. Adv. Mater. **8**, 170–172 (2007).
7. Y. Mori, K. Yamamura, K. Endo, K. Yamauchi, K. Yasutake, H. Goto, H. Kakiuchi, Y. Sano, and H. Mimura, "Creation of perfect surfaces," J. Cryst. Growth. **275**, 39–50 (2005).
8. B. J. Hamrock, S. R. Schmid, and B. O. Jacobson, *Fundamental of Fluid Film Lubrication* (Taylor & Francis, 2004), pp. 91–97.

9. P. Yang and S. Z. Wen, "A generalized Reynolds equation for non-Newtonian thermal elastohydrodynamic lubrication," J. Tribol. **112**, 631–636 (1990).
10. D. Zhu and S. Z. Wen, "A full numerical solution for the thermal elastohydrodynmaic problem in elliptical contacts," J. Tribol. **106**, 246–254 (1984).
11. S. F. Soares, D. R. Baselt, J. P. Black, K. C. Jungling, and W. K. Stowell, "Float-polishing process and analysis of float-polished quartz," Appl. Opt. **33**, 89–95 (1994).
12. Y.-T. Su, S.-Y. Wang, and J.-S. Hsiau, "On machining rate of hydrodynamic polishing process," Wear **188**, 77–87 (1995).
13. Y.-T. Su and Y.-C. Kao, "An experimental study on machining rate distribution of hydrodynamic polishing process," Wear **224**, 95–105 (1999).
14. M. Kaneta, H. Nishikawa, K. Kameishi, T. Sakai, and N. Ohno, "Effects of elastic moduli of contact surfaces in elastohydrodynamic lubrication," J. Tribol. **114**, 75–80 (1992).